

PRELIMINARY TESTS OF PIEZOELECTRIC AND MAGNETIC FAST STEERING MIRRORS P-FSM150S AND M-FSM45 FOR LARGE SCALE FSO CONSTELLATIONS

G. Aigouy⁽¹⁾, A. Guignabert⁽¹⁾, E. Betsch⁽¹⁾, H. Grardel⁽¹⁾, P. Personnat⁽¹⁾, J.M Nwesaty⁽¹⁾, X. De-Lepine⁽¹⁾, A. Bedek⁽¹⁾, A. Baillus⁽¹⁾, N. Bourgeot⁽¹⁾, F. Claeysen⁽¹⁾, R. Greger⁽²⁾, P. Lombardi⁽²⁾, A. Casciello⁽²⁾,

⁽¹⁾ CEDRAT Technologies, 59 ch. du vieux Chêne, 38240 Meylan, France, Email: gerald.aigouy@cedrat-tec.com

⁽²⁾ ThalesAlenia Space, Schaffhauserstrasse 580 8052 Zürich, Switzerland Email: ralf.greger@thalesalieniaspace.com

ABSTRACT

New space giant constellations based on Free-Space Optical Communication (FSO) are a new challenge from many perspectives. Considering the mandatory cost efficiency, with repeatability of performances, and reliability with no defect at customer integration, requires an upheaval in space production and acceptance test methods, when the quantities are beyond several thousands of units.

In this publication CEDRAT TECHNOLOGIES (CTEC) presents the test results of the P-FSM150S Pointing Ahead Mechanism (PAM) and M-FSM45 Fast Steering Mirror (FSM) Engineering Models, developed under ARTES project TELCO-B for future FSO constellations. The cost-efficient hardware design is presented, dedicated to very large quantities to be manufactured, together with the performance test results over a preliminary batch of EM's production.

P-FSM150S & M-FSM45 SIC MIRRORS

Two mirrors have been designed and tested for both the P-FSM150S and M-FSM45. Both mirrors have been designed in silicon carbide (SiC) material, according to CTEC heritage on NASA/PSYCHE PAM30 project [1,2], and have been successfully tested before and after integration on each mechanisms.

Mirror design

One of the main design constraints of an embedded optics mechanism is to keep the mirror surface deformation to a minimum to limit the induced optical wave front error below the requirements. On this case, a maximum of 40nm rms RWE at 0° mirror surface flatness is the target (corresponding to a 20nm rms optical surface flatness).

To ensure that the specification would be reached, CTEC used tools developed for previous space optical mechanisms projects. Specifically including evaluation of induced surface deformation caused by mechanical biases, thermal deformation as well as optimisation of mirror shape and dimensions.

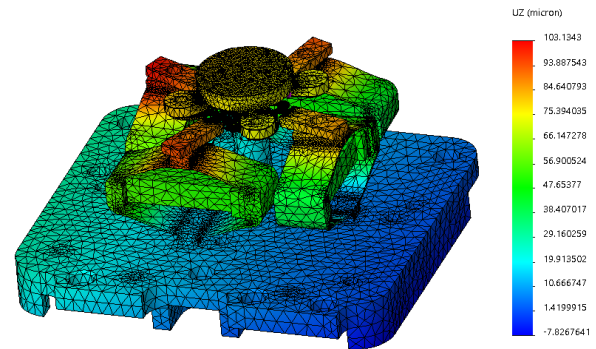


Figure 1: P-FSM150S simulation (vertical displacement) for a +60°C temperature

The design optimization process included not only the mirror, but also an equally important part, the mirror support. The mirror support is the part ensuring the mechanical link between the actuators and the mirror. To greatly limit the mechanical deformation transmitted to the mirror from the mechanism distortions, CTEC developed a dedicated flexible mirror support.

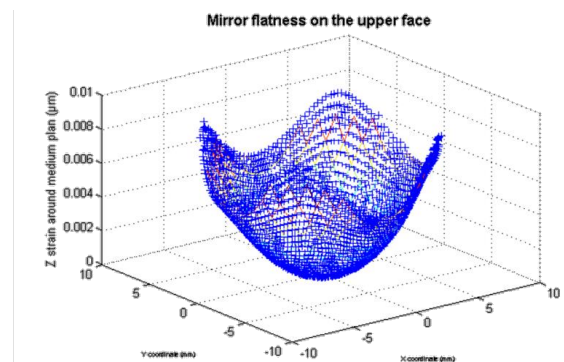


Figure 2: mirror deformation for a +60°C temperature

For both mechanisms, a specific mirror and support design was performed. The design aimed at reducing the operational optical surface deformation, while keeping the assembly stiff enough to withstand (mechanical stress considerations) environmental conditions (temperature, vibrations) and mechanisms forces.

The mirror deformation induced by the mechanism was targeted to be under 20nm rms RWE, the mirror manufacturer was requested to deliver a mirror with a coated mirror also under 20nm rms RWE.

Mirror procurement and verification

The 2 mirrors were manufactured for the engineering models (3 EM's of each) and optical verifications were performed.

The following pictures shows the mirrors on the RWE (reflected wave front error measured with Zygo interferometer at CTEC laboratory).

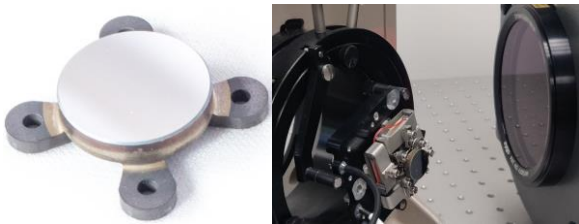


Figure 3: Free state mirror (left) and Mirrors RWE test after integration (right)

After both mechanism assembly (P-FSM150S and M-FSM45), the mirror surface flatness was controlled:

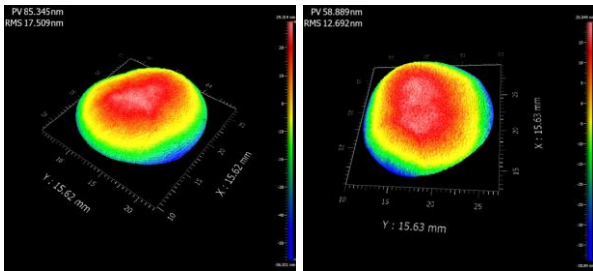


Figure 4: Mirrors RWE after integration M-FSM45 (left) P-FSM150S (right)

The optical verification indicates that both mirrors are compliant with important margins in both free state and after integration. The RWE of M-FSM45 mirror is a bit better than the P-FSM150S because its mirror is thicker.

Table 1: mirror optical control results (specification: RWE < 40nm rms)

| | P-FSM150S | M-FSM45 |
|--|-----------|---------|
| Mirror RWE before integration (nm rms) | 14.2 | 10 |
| Mirror RWE after integration (nm rms) | 17.5 | 12.7 |

P-FSM150S POINT AHEAD MECHANISM (PAM)

The main specifications for this mechanism were to ensure an angular stroke of +/-7 mrad throughout the full operational temperature range of the mission (-10/+60°C) and a mirror surface flatness under 40nm rms RWE (Reflected Wavefront Error) while remaining inside a very limited volume (especially less than 30mm height) and surviving launch vibrations.

Mechanism overview

The piezo actuators are cabled in 2 push-pull configurations (1 per axis) to allow a direct mirror rotation control, inheriting from PHARAO and ATLID tip-tilt mechanisms [3,4].

The P-FSM150S itself is composed of the following parts:

- A bracket baseplate (in aluminium): The APA® (Amplified Piezo Actuators) are fixed on it with screws.
- 4 APA® (in stainless steel): They provide the required displacement and are fixed to the baseplate and to the mirror support. The APA® are equipped with SG sensors by gluing process
- A mirror support (in stainless steel) which holds the mirror. It includes flexible parts in order to ensure a guiding function (to control the centre of rotation) while limiting the mirror deformation (insulate the mirror surface from the mechanism bias)
- A guiding blade (in titanium) soldered onto the central cylinder that stiffens the assembly.
- A Silicon Carbide (SiC) substrate-based mirror from Mersen OptoSiC®



Figure 5: PFSM-150S Engineering Model N°1

Strain Gauge position sensors (SG)

In order to be able to monitor the mirror angle, an indirect solution using strain gages placed on each piezo actuator is selected, based space heritage from other projects,

especially ATLID [4] on this matter, which enabled an important development on SG assembly process. The project used constantan, 350Ohm SG. There is 1 SG per piezo stack, mounted in one full Wheatstone bridge per rotation axis to maximize the sensitivity while minimizing thermal drift. All SG wires and PCB traces are the same length to limit offset drift.

New APA® piezo actuator design

The mechanism is composed of 4 APA®, deriving from CTEC standard APA120S. The existing CTEC actuators were either slightly too short in stroke or not stiff enough to ensure the mechanism survival during the launch. Therefore APA150S have been specifically designed for the application needs.

A total of 25 APA® were assembled and tested, the measurements are detailed in the following table:

Table 2: P-FSM custom APA measurement results

| | Full stroke (-20/+150V) | 1st coupled resonant frequency |
|--|-------------------------|--------------------------------|
| | µm | Hz |
| Average (measured) | 187.3 | 4892.0 |
| Standard deviation (measured) | 0.9 | 22.9 |
| Design value (worst case) | 152.8 | 4783 |
| Difference measurement/design value | +23% | +2% |

P-FSM150S assembly

At the time of June 2021, two P-FSM150S EM have been assembled (EM1 and EM2). The integration process and assembly tooling was constantly improved as the operations were progressing. Even for prototypes, one of the focus was to keep the time required to assemble the model as low as possible, in anticipation with the aim to have this mechanism compatible with serial production.

Hence the number of steps, especially highly time-consuming ones like gluing, was reduced to the minimum required without impacting required quality.

With that in mind, each integration step duration was monitored and the overall process time was analysed in order to identify critical steps and room for process optimization.

P-FSM150S preliminary test results

The two breadboards are currently under test but some preliminary results are presented in this paper.

Stroke

As it was anticipated based on the good piezo actuators stroke performance (see Table 2), the P-FSM150S mirror tilt angle range is compliant with the requirements, with notable operational margins. Hence the target stroke of +/-7mrad can even be reached (at ambient temperature) supplied with a limited voltage range of 0/+130V instead of -20/+150V (23% less voltage).

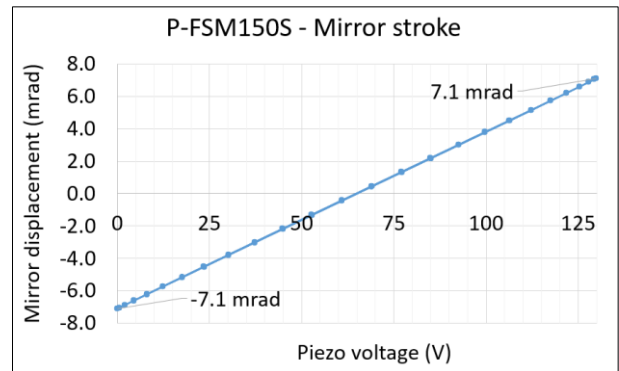


Figure 6: PFSM150S stroke results with a 0/+130V supply

The actual full operational stroke could not be fully tested due to the limited range of the autocollimator instrument, but we can extrapolate that the PFSM could reach a +/-9.6mrad stroke with a -20/+150V supply, which should cover the slight stroke loss expected in cold operational temperature (around -5%) and the mirror integration offset compensation.

Modal landscape

The mechanism stiffness and associated modal landscape is evaluated with an admittance sweep. With that method, only the piezo coupled modes are visible, hence the vertical pumping mode (cancelled from piezo point of view) is not visible.

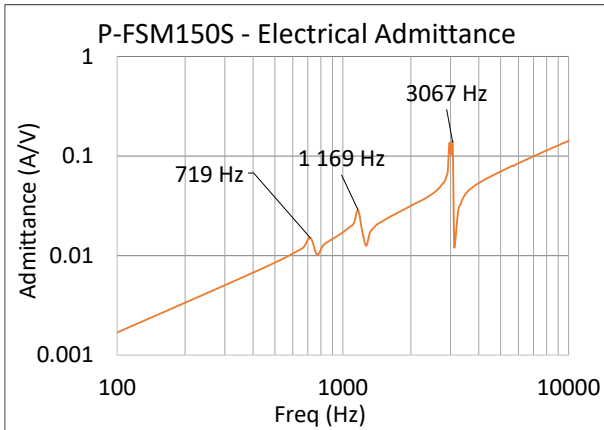


Figure 7: PFSM150S EMI X-axis admittance sweep

The first mode measured at 719Hz corresponds to the X axis mirror tilt, the main actuation mode. The modal simulations results evaluated the tilt modes at 738Hz, the result is then quite close to the simulation (-2.6%), the difference coming from model approximations, material uncertainties and parts machining tolerances.

Mechanism accuracy performances

The tests reveal a 0.1% cross coupling: $\pm 10\mu\text{rad}$ cross axis displacement with a $\pm 7\text{mrad}$ stroke which is a good result given the high amplification of the mechanism.

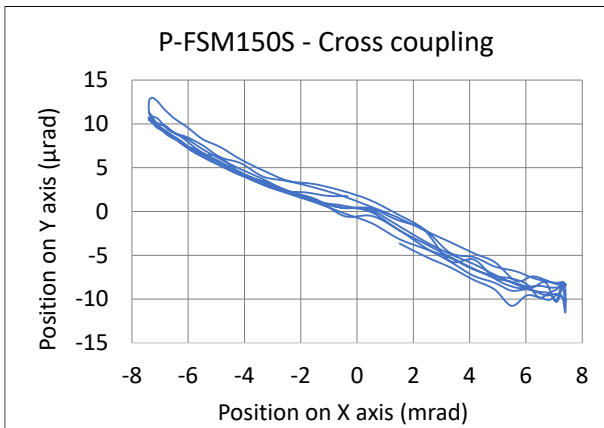


Figure 8: PFSM150S cross coupling measurement

With another test, it is demonstrated that the mechanism can generate $\pm 1\mu\text{rad}$ steps (0.01% mechanical resolution), using an external measurement for the mirror angle (autocollimator). The share of errors due to instruments measurement has still to be determined (especially for cross coupling) but measured resolution is already compliant with the $\pm 1\mu\text{rad}$ specification.

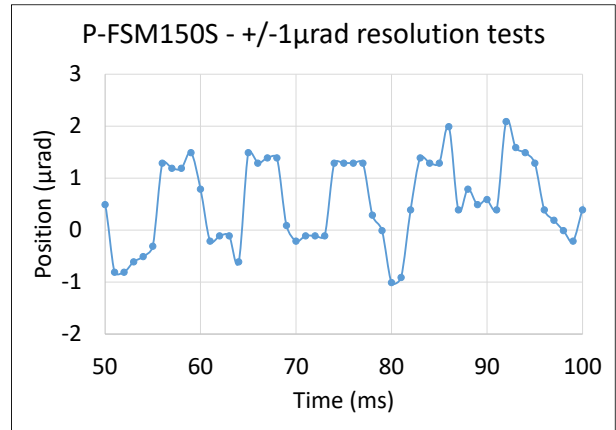


Figure 9: mechanical resolution test

Ongoing accelerated fatigue lifetime test

The EM1 is currently going through a lifetime test. The mechanism is actuated at full stroke ($\pm 7\text{mrad}$) in diagonal direction (45° along x and Y axis) to excite both axis in fatigue. With a frequency of 100Hz, 2.6e8 cycles are performed each month so the first billion cycles will be reached after almost 4 months of tests.

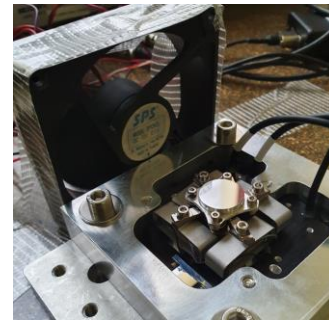


Figure 10: lifetime test set-up for PFSM150S EMI

The lifetime test will be regularly interrupted to perform stroke and SG verification, to detect any deviation linked to lifetime evolution.

M-FSM45 FAST STEERING MIRROR (FSM)

Mechanism overview

The M-FSM45 is a magnetic mechanism driving two tilt axis on a large angle requirement. This FSM, which derives from M-FSM62 [5,6] is composed of the following parts :

- A Magnetic circuit in Soft Magnetic Composite material with 4 magnets and a moving part.
- 4 Coils optimized to provide the best induction in the short volume, with potting to dissipate the generated heat.
- An Eddy Current Sensor device with aluminium targets embedded on the moving parts, and 4

sensing heads on a single PCB below.

- A moving part suspended on a flexure bearing ensuring high lifetime performances.
- A mirror fixed on a flexible baseplate limiting the integration deformations.

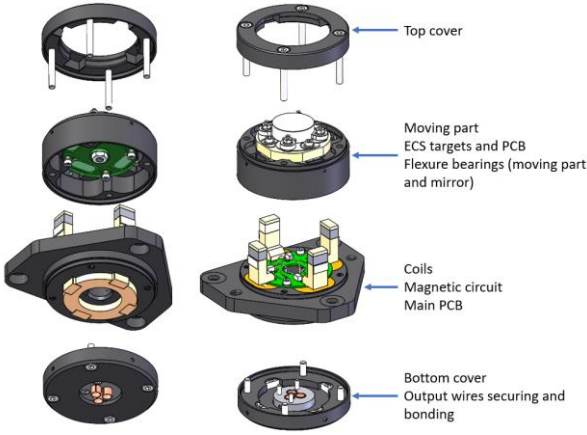


Figure 11: M-FSM cost efficient design concept

Magnetic design

The magnetic design relies on forces due to tangential variable magnetic reluctance, which offers higher forces than Lorentz forces [7] and more linear forces than normal variable magnetic reluctance [8].

To ensure the FSM performances, magnetic calculations by FEA have been performed. The magnetic saturation, available torque and parasitic forces were verified.

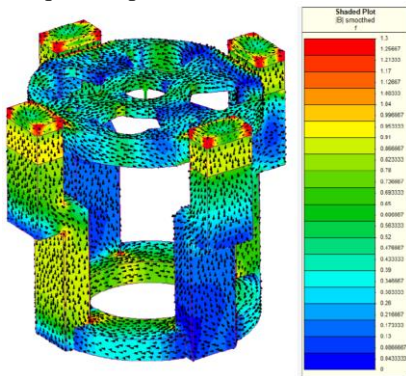


Figure 12: M-FSM Magnetic Finite Element Analysis

The magnetic circuit is created through powder metallurgy process, limiting the perturbation effects of eddy currents. The available geometrical tolerances were anticipated to sustain the worst case air gaps in the torque calculation.



Figure 13: M-FSM SMC parts

Eddy Current position Sensors (ECS)

To measure the mirror position and perform closed loop control, an eddy current sensor assembly is embedded in the mechanism. The sensor assembly is eased thanks to the design of a single PCB including the 4 sensing coils, taking advantage of space qualification of PCB-ECS sensors [9]. This solution makes the M-FSM more compact, with an efficient one step assembly. The sensitivity has been optimised for the FSM stroke, making sensor the non-linearity a key parameter which should be in line with the common values of the ECS solutions.

M-FSM45 EM N°1 Assembly

The assembly of the mechanism has been performed with the aim of reducing the complex steps in order to be efficient for a large number of mechanisms production. Specific tooling were designed for critical steps as mirror assembly, coils potting or moving part insertion in the magnetic circuit.

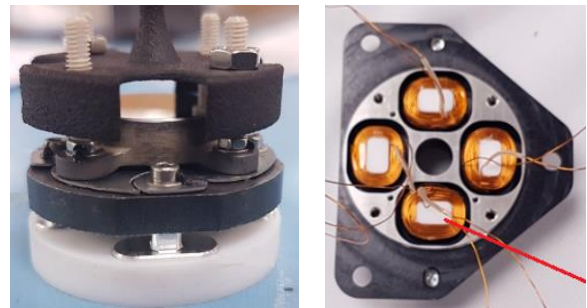


Figure 14: M-FSM45 tooling for mirror and moving part assembly (left) and coils potting (right)

The final integration is shown in the following pictures.



Figure 15: M-FSM45 Engineering Model N°1

M-FSM45 EM preliminary test results

The M-FSM performances have been measured in open-loop to validate the available stroke, frequency and coils values.

As expected, the first resonance frequency is located around 100Hz. The calculated coils parameters are validated through the impedance and inductance measurements.

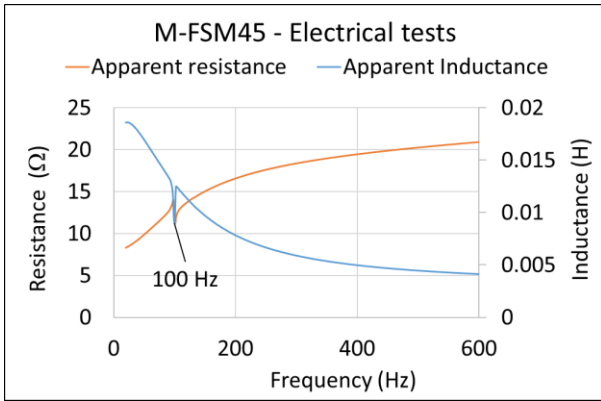


Figure 16: M-FSM45 electrical tests

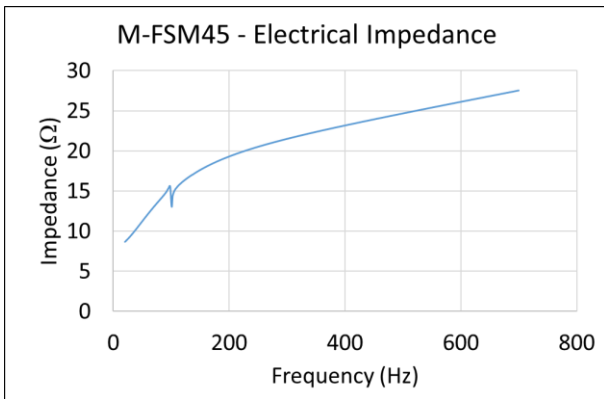


Figure 17: M-FSM45 Electrical impedance

The stroke measured shows that the M-FSM is allowing a maximal stroke slightly lower than $\pm 1.5^\circ$ ($\pm 25.8\text{mrad}$) for a $\pm 1\text{A}$ current input. The measurements have been performed thanks to a large angle autocollimator allowing a single angle low frequency acquisition

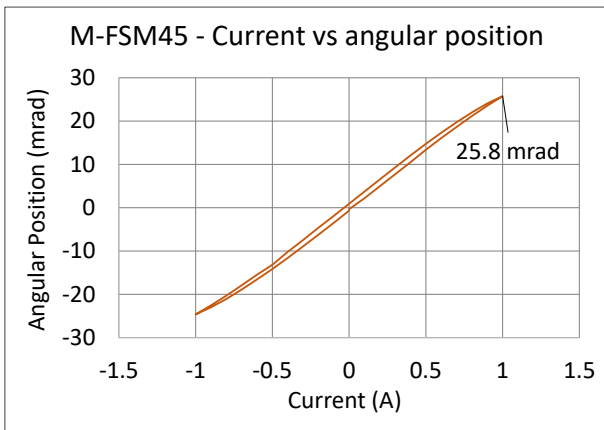


Figure 18: M-FSM45 stroke amplitude test

M-FSM45 closed loop position control development

The development of the position feed-back closed loop control on the M-FSM technology, is currently under

development and test onto the M-FSM62, and is soon to be implemented and tested onto the M-FSM45. The presented position feed-back control of M-FSM's is based on the embedded ECS position sensors.

The test with closed loop control allows to measure the mechanical performances, as well as all the electrical driving performances, with drive electronics having representative limits w.r.t flight ones, in terms of voltage, current, power, and closed loop controller tuning.

The following results presented here after for the M-FSM62 are expected to be representative of the M-FSM45, with much lower power consumption rated on the M-FSM45, as well as miniaturisation as summarised in the following table.

Table 3: M-FSM62 tests & M-FSM45 expected results

| | Tested on M-FSM62 | Expected on M-FSM45 |
|------------------------------------|---------------------------|---------------------------|
| Mirror aperture | 30mm | 15mm |
| Diameter | 62mm | 46mm |
| Height | 56mm | 35mm |
| Mass | 400g | 195g |
| Stroke amplitude | $\pm 50\text{mrad}^{(1)}$ | $\pm 15\text{mrad}^{(2)}$ |
| Resonance freq. | 100Hz | 100Hz |
| Max. rated voltage | 40V | 12V |
| Max. rated current | 10A | 0,5A |
| Max. rated power for freq. < 100Hz | 2,5W | 2,5W |
| Max. rated power for freq. > 100Hz | 50W | 2,5W |
| -3dB Bandwidth @ Full stroke | 145 Hz | 145 Hz |

(1) Reduced to $\pm 25\text{mrad}$ with embedded ECS position sensor option.
(2) Successfully tested up to $\pm 25\text{mrad}$ with 1A current.

The following picture shows the closed loop position feed-back test bench, using both internal ECS position sensors and external optical instrumentation (autocollimator and PSD) using a laser pointing source.



Figure 19: M-FSM62 on optical test bench

The M-FSM62 frequency bandwidth could be measured at several stroke amplitudes, up to $\pm 25\text{mrad}$, and one can see that -3dB bandwidth was measured at 146Hz.

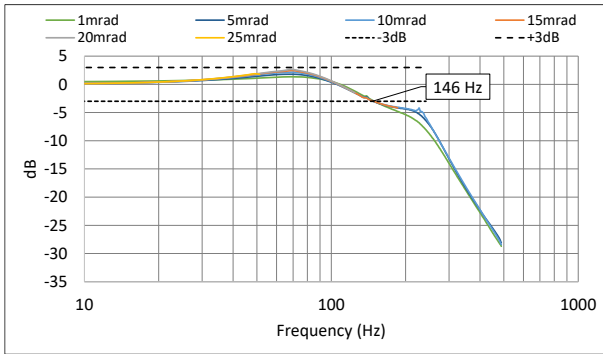


Figure 20: Bandwidth tests at different amplitudes.

The drive electronic used for the test was the MCSA480 which provides a maximum current rated at 10A, with safety hardware shut down beyond. The following picture shows the stroke amplitude that was achievable versus frequency up to the reaching of maximum limit of electronic shut down (hardware shut down curve).

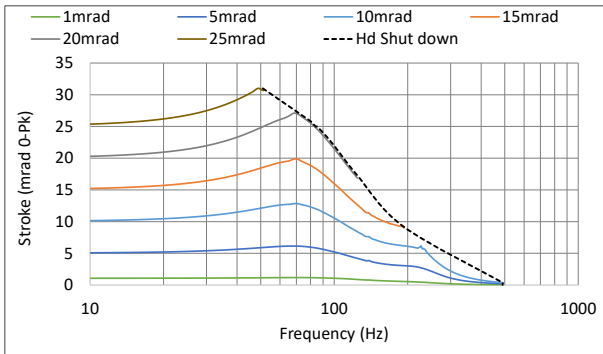


Figure 21: M-FSM62 Amplitude diagrams v.s electronics limits.

The advantage of the MCSA480 is its high electrical power rating, which allows testing a magnetic FSM far beyond its resonance frequency and at high power. This result is of high interest, because the required power in order to achieve high stroke at frequencies higher than the resonance frequency dramatically increases. One can see in the following plot that +/-25mrad at 50Hz driving frequency requires only 2,5W on the M-FSM62, whereas driving frequencies higher than 200Hz requires about 50W for maximum reachable stroke amplitude about +/-6mrad.

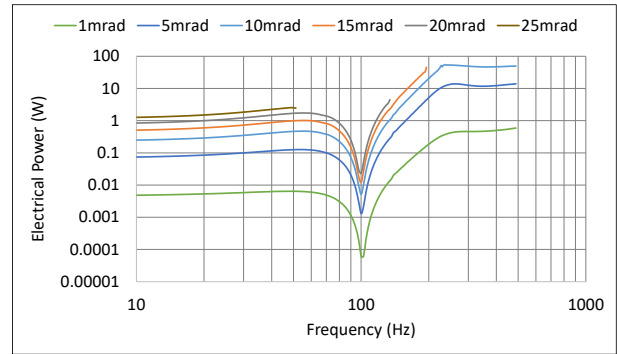


Figure 22: Power diagrams at different amplitudes.

The measured electrical active power absorbed by the M-FSM62, was analysed in coil Joule effect, and in Eddy currents losses, which result both in heating onto the M-FSM. This analysis here under shows the results for a stroke amplitude of +/-10mrad, which is considered as relevant target for flight. One can see that under 100Hz the total electrical active power absorbed is lower than 0,5W with Eddy currents losses increasing versus frequency, and becoming comparable to coil Joule losses for frequencies beyond 100Hz, leading to 50W total power consumption at 200Hz with +/-6mrad of stroke achievable. This illustrates the power effort required for the driving of a magnetic FSM far beyond its resonance frequency, which is not a trivial result.

The M-FSM45 mirror and moving mass being much smaller compared to M-FSM62, and together with a better optimisation w.r.t Eddy current losses (shape and materials) the M-FSM45 power consumption at high frequency is expected to be much smaller.

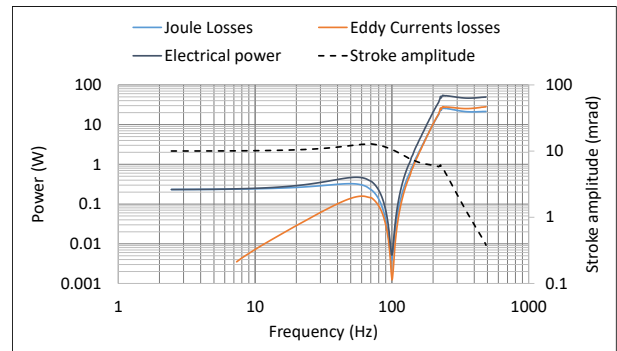


Figure 23: Power diagrams at +/-10mrad amplitude.

Acknowledgement and conclusion

This development was achieved during the TELCO-B ARTES project under the funding of CNES and ESA. The authors particularly thanks Thales Switzerland, CNES and ESA, which have allowed the bringing to maturity of P-FSM150S and M-FSM45 as candidate flight products for future large-scale space constellations.

References

1. A. Guignabert, Point Ahead Mechanism for Deep Space Optical Communication for PSYCHE mission, Proc. ICSO, February 2021
2. A. Guignabert, Point Ahead Mechanism for Deep Space Optical Communication – Development of a new Piezo-Optical Tip-tilt mechanism, Proc AMS, Houston, May 2020
3. R. Le Letty, Miniature Piezo Mechanisms for Optical and Space applications, ACTUATOR Conf, Messe Bremen (G), June 2004, pp 177-180
4. F. Claeysen, Beam Steering Mirrors from space applications to optronic solutions, Proc. OPTRO Conf, Paris, Feb. 2018
5. F. Claeysen, Large-stroke Fast Steering Mirror for space Free-Space Optical communication, OPTRO 2020, n°0062, 28-30 Jan 2020
6. A. Guignabert, E. Betsch, G. Aigouy, Large stroke Fast Steering Mirror, Proc. ICSO, February 2021
7. W. Coppolse, Dual-axis single-mirror mechanism for beam steering and stabilisation in optical inter satellite links, Proc ESMATS conf, 2003
8. Y. Long, Design of a Moving-magnet Electro magnetic Actuator for Fast Steering Mirror, J. of Magnetics, Vol. 19 (3), 2014
9. JC Barriere, Qualification of euclid-near infrared spectro-photometer cryomechanism, Proc. ESMATS 2017